Supplementary Information

Dependence on co-adsorbed water in the reforming reaction of ethanol on Rh(111) surface

Yu-Yao Hsia[a], Po-Cheng Chien[b], Lu-Hsin Lee[a], Yu-Ling Lai[c], Yao-Jane Hsu[c], Jeng-Han Wang[b,*] and Meng-Fan Luo[a,*]

[a]*Department of Physics, National Central University, No. 300 Jhongda Road, Jhongli District, Taoyuan 32054, Taiwan*

[b]*Department of Chemistry, National Taiwan Normal University, No. 88, Sec. 4, Ting-Zhou Road, Taipei, Taiwan*

[c]*National Synchrotron Radiation Research Center, 101 Hsin-Ann Road, Hsinchu Science Park, Hsinchu 30076, Taiwan*

Figure S1 shows the D_2O TPD spectra for 1.0- and 2.0-L D_2O adsorbed on Rh(111) surface at 120 K. For 1.0-L D_2O (lower one), a primary desorption feature was centered about 170 K, corresponding to monolayer D_2O on the surface; for 2.0-L D_2O (upper one), an additional desorption feature appeared about 150 K, attributed to multilayer D_2O. The desorption temperature of the monolayer D_2O on Rh(111) is about 25 K lower than that on $Rh(111)_{O*(0.08\ ML)}$, because on $Rh(111)_{O*(0.08\ ML)}$ D_2O* interacts with O* and a hydrogen-bonded network of D_2O* and OD* forms [1].

Figure S2(a) and (b) show the DHO (*m/z* = 19 u) TPD spectra from $Rh(111)_{O*(0.08\ ML)}$ exposed to D_2O of varied amounts (denoted as $Rh(111)_{D2O*/O*(0.08\ ML)}$) and to D_2O of varied amounts and subsequently 3.0-L ethanol. The desorption contained evident DHO signals largely because the D_2O exposure contained some DHO (monitored with mass spectrometer), formed on exchange of H and D of dosed D_2O and background H_2O. The desorption behavior of DHO resembles that of D_2O. With the co-adsorption of ethanol, the multilayer desorption feature of DHO was enhanced ((a) and (b)), since adsorbed ethanol diffused toward the Rh(111) surface and exchanged position with underlying DHO. Figure S2(c) plots the integrated intensities of the DHO desorption features in (a) and (b) as a function of D_2O exposure. It is noted that the DHO signals from the sample with ethanol (red) were constantly greater than those without ethanol (black). The greater DHO signals from co-adsorbed ethanol arise from an additional

channel: surface OD* (from $D_2O^* + O^* \rightarrow 2OD^*$ and $DHO^* + O^* \rightarrow OD^* + OH^*$) abstracted H from ethanol and desorbed as DHO.

Figure S3 plots the total adsorbed ethanol (denoted as $ethanol_{(t)}$), measured with the integrated intensities of the corresponding desorption features, as a function of D_2O exposure. The $ethanol_{(t)}$ contains ethanol in multilayer regime and $ethanol_{(int)}$; the $ethanol_{(int)}$ consisted of those adsorbing directly on Rh(111) surface and those migrating from top D_2O overlayers to the D_2O-Rh(111) interface to react or desorb, so contained desorbing and decomposing ethanol at the Rh(111) surface. The $ethanol_{(t)}$ decreased with increasing D_2O overlayers primarily because of a smaller sticking coefficient onto D_2O overlayers than that onto Rh(111) surface. The decreasing trend of $ethanol_{(t)}$ resembles in general that of $ethanol_{(int)}$ (Figure 2(d)); the latter decreased slightly more than the former as the D_2O overlayers obstructed a little the diffusion of ethanol toward the Rh surface.

Figure S4 shows D_2 and DH TPD spectra from $Rh(111)_{O^*(0.08\ ML)}$ exposed to D_2O of varied amounts (0, 1.0 and 4.0 L) and subsequently 3.0-L ethanol. Both D_2 and DH signals were very small, amounting roughly to 1 – 2 % that of H_2 signals. The result implies few D* and hence limited dissociation via $D_2O^* \rightarrow OD^* + D^*$; the OD* was produced primarily through $D_2O^* + O^* \rightarrow 2OD^*$.

Figure S5 shows schemes for the decomposition of $CH_3CH_2O^*$, producing (a)

CH_2CH_2, (b) **CO**, (c) **CH_4** and (d) **H_2**. It is presented here as a complement for Figure 5. The corresponding energies of $\Delta E/E_a$ on clean Rh(111) and $Rh(111)_{OH*}$ surfaces are shown in blue and red numbers (in eV), respectively.

Table S1 compares the calculated energies (E_{ads}, ΔE and E_a) in the present work and previous studies. They exhibit similar values and trends.

References

[1] A.E. Shavorskiy, T. Eralp, E. Ataman, C. Isvoranu, J. Schnadt, J.N. Andersen, G. Held, Dissociation of Water on Oxygen-Covered Rh{111}, J. Chem. Phys., 131 (2009) 214707.

Figure S1

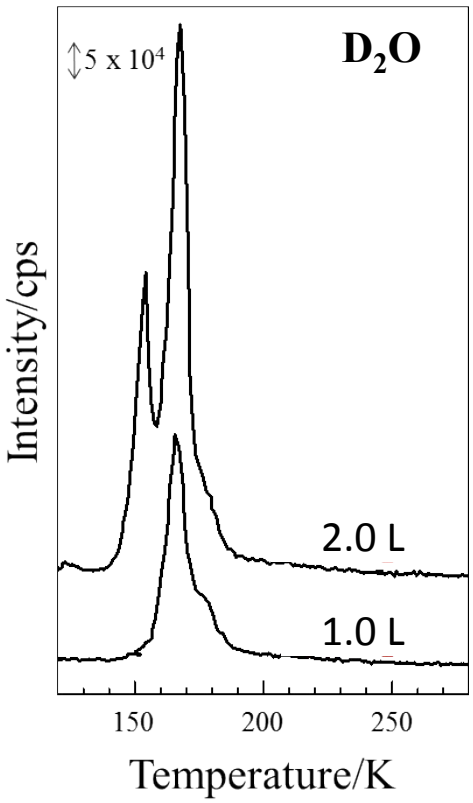

Figure S1 D_2O TPD spectra from Rh(111) exposed to 1.0- and 2.0-L at 120 K.

Figure S2

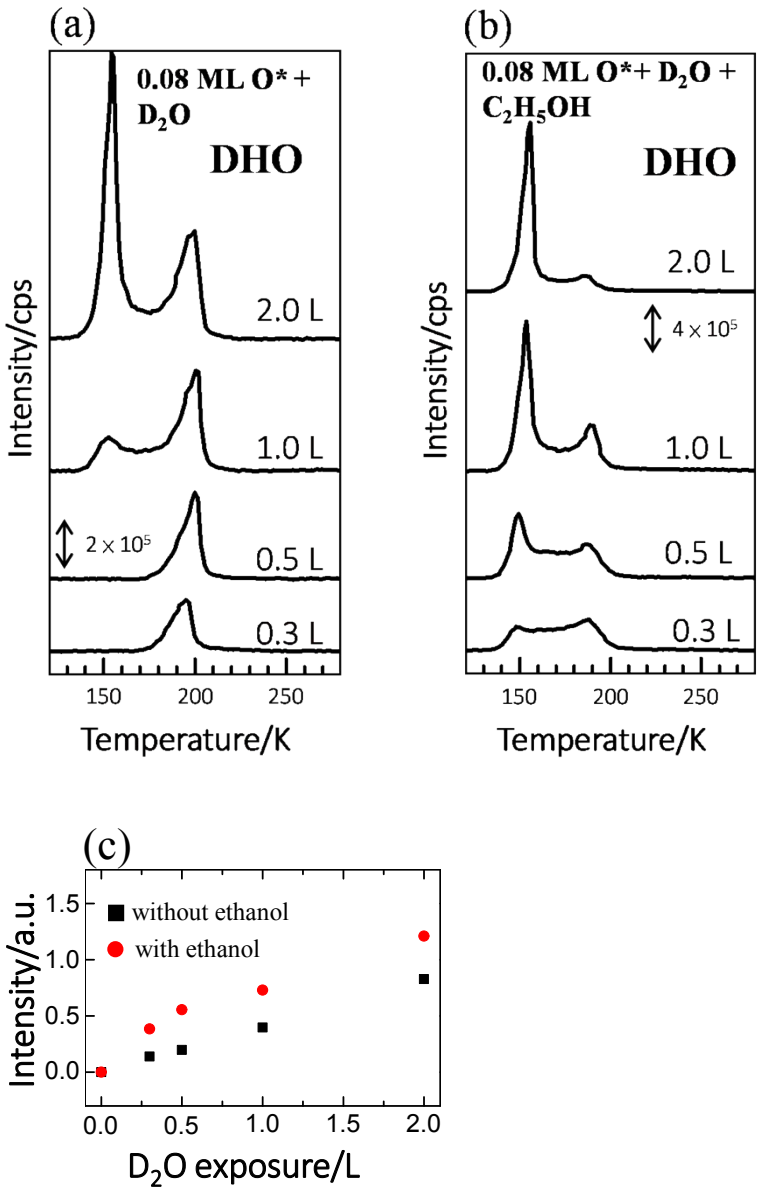

Figure S2 DHO TPD spectra from $Rh(111)_{O^*(0.08\ ML)}$ exposed to (a) D_2O of varied amounts, as indicated, and to (b) D_2O of varied amounts and subsequently 3.0-L ethanol. (c) plots the integrated intensities of the DHO desorption features in (a) and (b) as a function of D_2O exposure; black squares and red spheres denote the data from the sample without and with ethanol, respectively.

Figure S3

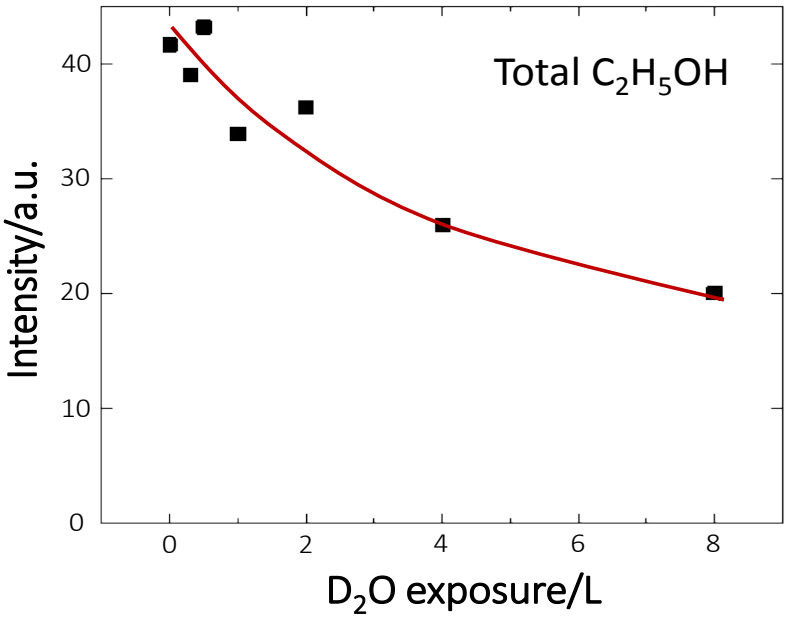

Figure S3 the quantity of total adsorbed ethanol as a function of D_2O exposure. The red line is drawn to guide the eyes.

Figure S4

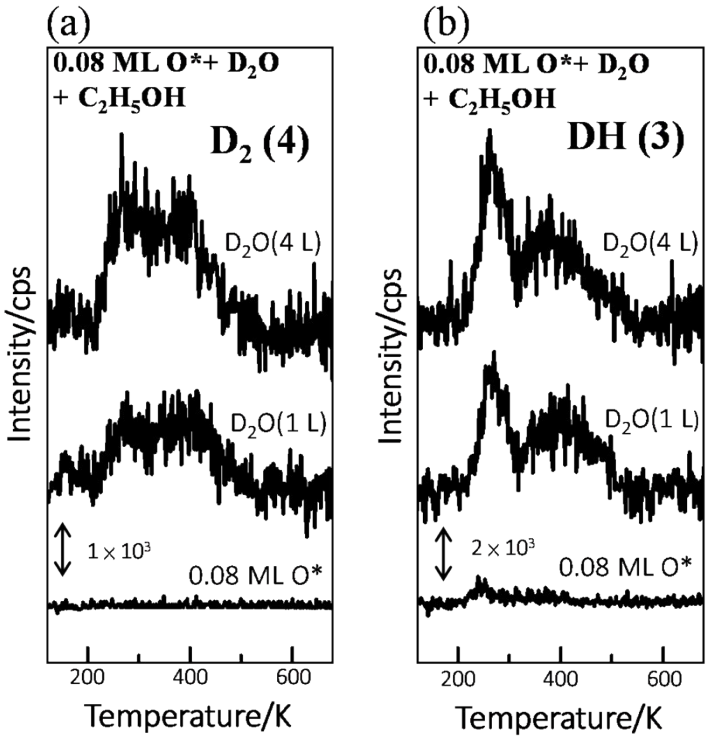

Figure S4 (a) D_2 and (b) DH TPD spectra from $Rh(111)_{O^*(0.08\ ML)}$ exposed to D_2O of varied amounts, as indicated, and subsequently 3.0-L ethanol.

Figure S5

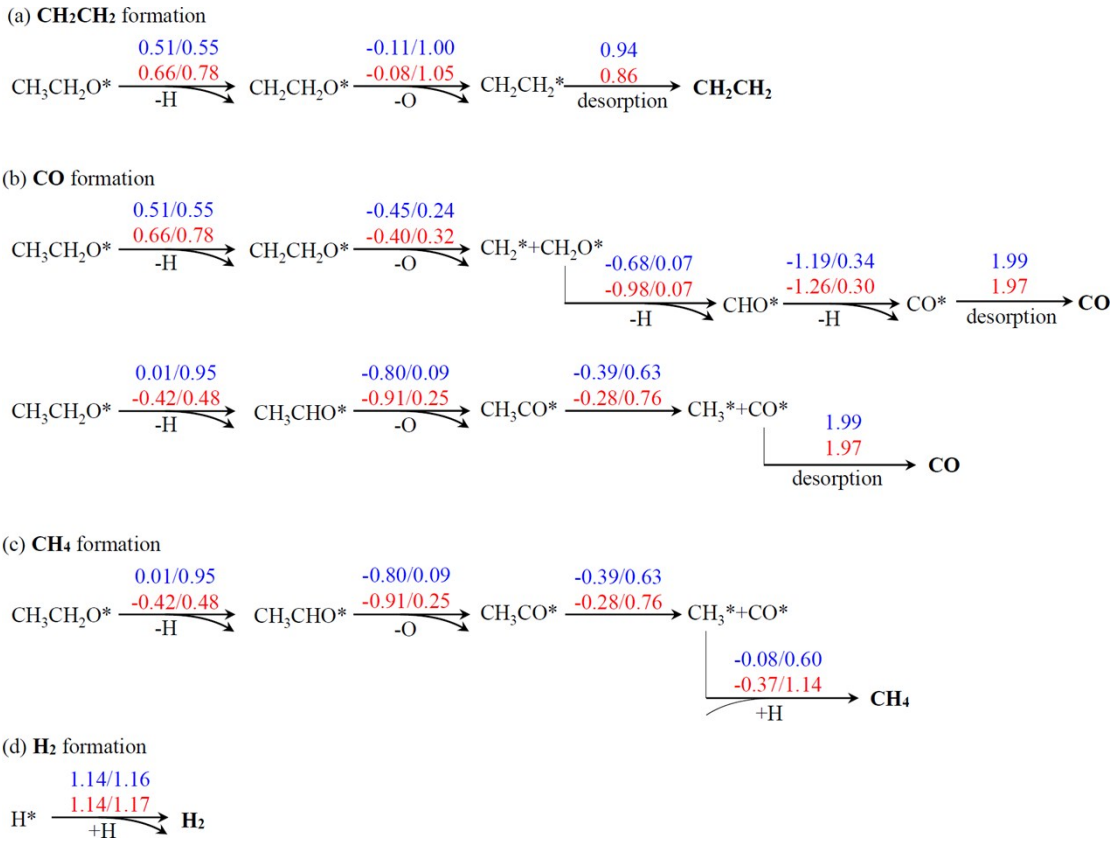

Figure S5 Schemes for CH_3CH_2O* decomposition forming (a) $\mathbf{CH_2CH_2}$, (b) **CO**, (c) $\mathbf{CH_4}$ and (d) $\mathbf{H_2}$, as a complement for Figure 5. The corresponding energies of $\Delta E/E_a$ on clean Rh(111) and OH* covered $Rh(111)_{OH*}$ surfaces are shown in blue and red numbers (in eV), respectively.

Table S1 Energy (E_{ads}, ΔE and E_a) comparison of the present work and previous studies.

	Present	Ref. 8	Ref. 21	Ref. 32	Ref. 33	Ref. 42
E_{ads} comparison						
$H_2O \rightarrow H_2O^*$	-0.37		-0.27			
$CH_2CH_2 \rightarrow CH_2CH_2^*$	-0.94					
$CO \rightarrow CO^*$	-1.99	-1.84	-1.70			
$CH_3CH_2OH \rightarrow CH_3CH_2OH^*$	-0.32	-0.46	-0.28	-0.46	-0.45	-0.59
ΔE and E_a comparison						
$O^*+H_2O^* \rightarrow 2OH^*$	0.20/0.98					
$CH_3CH_2OH^*+OH^* \rightarrow CH_3CH_2O^*+H_2O^*$	-0.66/0.23					
$CH_3CH_2OH^* \rightarrow CH_3CH_2O^*+H^*$	-0.19/0.58	0.03/0.75		-0.19/0.82	0.82/0.11	-0.15/0.74
$CH_3CH_2O^* \rightarrow CH_2CH_2O^*+H^*$	0.51/0.55	0.52/0.96				
$CH_3CH_2O^*+OH^* \rightarrow CH_2CH_2O^*+H_2O^*$	0.66/0.78					
$CH_2CH_2O^* \rightarrow CH_2CH_2+O^*$	-0.11/1.00	-0.08/0.90				
$CH_2CH_2O^* \rightarrow CH_2^*+CH_2O^*$	-0.45/0.24	-0.67/0.93				
$CH_2O^* \rightarrow CHO^*+H^*$	-0.68/0.07		-0.39/0.09			
$CHO^* \rightarrow CO^* + H^*$	-1.19/0.34		-1.03/0.32			
$CH_3CH_2O^* \rightarrow CH_3CHO^*+H^*$	0.01/0.95	-0.07/1.43			0.00/0.67	
$CH_3CHO^* \rightarrow CH_3CO^* + H^*$	-0.80/0.09		-1.08/0.06			-0.50/0.69
$CH_3CO^* \rightarrow CH_3^* + CO^*$	-0.39/0.63		0.15/0.93			-0.64/0.15
$CH_3^*+H^* \rightarrow CH_4$	-0.08/0.60	-0.49/0.58	-0.20/0.57			-0.20/1.18
$2H^* \rightarrow H_2$	1.14/1.16					